

# Subsonic-Transonic Drag of Supersonic Inlets

GEORGE L. MULLER\* AND WILLIAM F. GASKO†  
Pratt & Whitney Aircraft, East Hartford, Conn.

The subsonic-transonic drag of supersonic inlets appears to be a subject that has been largely neglected in the transition from subsonic to supersonic design-point flight. Now that more emphasis is placed on off-design performance of supersonic aircraft, more information is required on this subject. Accordingly, experimental data were obtained on subsonic-transonic drag of two types of supersonic inlets. The types investigated were two-dimensional and axisymmetric plug inlets. The two-dimensional inlets were of the single-ramp mixed compression variety. The axisymmetric inlets had a conical plug and were also of the mixed-compression type. The range of variables studied was as follows: two-dimensional inlet ramp angle,  $6^\circ$ - $12^\circ$ ; axisymmetric inlet conical plug half-angle,  $10^\circ$ - $18^\circ$ ; two-dimensional inlet throat-capture area ratio, 0.32-0.80; and axisymmetric inlet throat-capture area ratio, 0.13-0.80. It was found that two-dimensional inlets have higher additive drags than axisymmetric inlets of the same area ratio and initial angle. This conclusion is the same as in supersonic flight.

## Nomenclature

$A_i$	= inlet flow area at cowl lip
$A_0$	= freestream tube area of captured flow
$A_1$	= inlet capture area
$A_2$	= inlet throat area (equal to $A_i$ for transonic-subsonic operation)
$C_{Dadd}$	= additive drag coefficient
$D_{add}$	= additive drag
$D_{cb}$	= centerbody pressure drag
$D_{ext}$	= external pressure drag
$D_f$	= friction drag
$F_A$	= net thrust available
$F_p$	= propulsion force exerted on aircraft
$F_{bal}$	= force on drag balance
$m_e$	= mass flow leaving exit
$m_i$	= mass flow entering cowl lip station
$m_0$	= mass flow in freestream tube enclosing captured flow
$M_0$	= freestream Mach number
$P_{ext}$	= external pressure
$\bar{P}_i$	= average pressure at cowl lip, $\int P dA/A$
$P_0$	= freestream pressure
$(PA)_{base}$	= force on base of drag balance
$(PA)_{step}$	= force on step between balance and model outer diameters
$\bar{v}_e$	= average velocity at exit, $\int v dm/m$
$\bar{v}_i$	= average velocity at cowl lip, $\int v dm/m$
$v_0$	= freestream velocity
$\gamma$	= ratio of specific heats of air

## Subscripts

$cb$	= centerbody
$e$	= exit station
$ext$	= external part
$i$	= inlet cowl station

## Introduction

IT is becoming increasingly important that the engine manufacturer be able to predict installed engine performance because installation penalties are more severe with today's high-performance aircraft. To minimize these penalties, installation effects, such as inlet correction factors, must be taken into account when engine cycles and designs

are determined. For example, additive drag—one of the inlet correction factors—could be changed by manipulating engine airflow requirements for off-design conditions. Knowledge of the gains to be made requires knowledge of levels of off-design additive drag.

The additive drag of supersonic inlets in the subsonic-transonic speed range appears to be a subject that has largely been neglected in the transition from subsonic to supersonic design-point flight. The state of available information on this subject was summed up by Mount.<sup>1</sup> Drag information on axisymmetric supersonic inlets did not exist, whereas some data on a Mach 2, two-dimensional, external compression inlet were available. The remaining information could only be analyzed by using the questionable assumption that the tare drag (obtained by adjusting the measured drag to zero at a mass flow ratio of 1.0) is unaffected by mass flow ratio.

As the subsonic performance requirements of supersonic aircraft increase, the need for drag data in this speed range becomes more acute. Unfortunately, in this speed range, it is difficult to compute inlet drag because of compressibility, shocks, flow curvature, and flow separation from sharp cowl lips. One-dimensional analysis usually fails to give more than qualitative trends. Accordingly, experimental measurements of drag must be made.

In this program, two common types of inlets were investigated. One type was a two-dimensional, single-ramp inlet with a sharp cowl. The other was an axisymmetric, conical plug inlet with a sharp cowl. A range of throat-capture area ratios and ramp or cone angles were investigated in order to be useful in inlet design studies. In addition, the captured flow rates were varied from zero to choked, and the Mach number from 0.5 to 1.3. Inlet drag data obtained from a 1959 test program<sup>2</sup> are also presented here. Axisymmetric, conical plug inlets with sharp cowls were tested as was done in the present program.

## Theoretical Considerations

The net propulsive force exerted on an aircraft is, by industry definition,

$$F_p = F_A - D_{add} - D_{ext} \quad (1)$$

Under this definition of force bookkeeping, net thrust available from the engine ( $F_A$ ) is supplied by the engine manufacturer. Additive drag  $D_{add}$  and external drag  $D_{ext}$  terms are evaluated by the aircraft manufacturer.

No system of force bookkeeping, however, can eliminate all interactions. For example,  $F_A$  depends on inlet pressure

Received October 7, 1966; revision received February 3, 1967. The major portion of this work was conducted for the United States Air Force Systems Command, Wright Patterson Air Force Base, under Contract AF33(657) 14903. [3.02, 4.02]

\* Assistant Project Engineer, Inlet Research and Technology. Member AIAA.

† Senior Engineer, Inlet Research and Technology. Member AIAA.

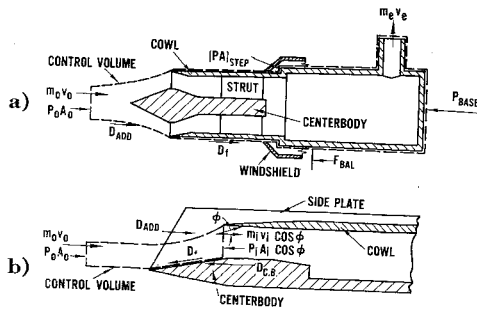


Fig. 1 Free body diagram for a) force model tests and b) pressure model tests.

recovery, inlet flow distortion, and local pressures at the engine exhaust. Also the exhaust gas flow can influence external drag.

### Additive Drag Concept

As a consequence of the force bookkeeping system, additive drag ( $D_{add}$ ) accounts for forces involved in bringing air from freestream conditions to the inlet cowl station  $i$ . It can be shown that additive drag is the external pressure-area integral over the stream tube ahead of the inlet, so that

$$D_{add} = \int_{O_{ext}}^i (P_{ext} - P_0) dA \quad (2)$$

### Additive Drag Theory

Equation (2) can be evaluated by assuming quasi-one-dimensional, isentropic flow for subsonic operation and one-dimensional flow with normal shocks for transonic (shock detached) operation. This theory has been shown to be accurate for pitot inlets at all mass flow ratios by Sibulkin.<sup>3</sup>

At high captured flow rates and high throat-capture area ratios, the theory can be extended to inlets with centerbodies because flow curvature is a minimum under these conditions and centerbody pressure forces can be approximated by the average pressure between freestream and the inlet throat.

Under other conditions, assumptions used in the theory are grossly violated, and results do not agree with experimental data. In fact, it will be shown that two-dimensional inlets have a higher measured drag than axisymmetric inlets of the same initial centerbody angle and area ratio, whereas the theory predicts no difference.

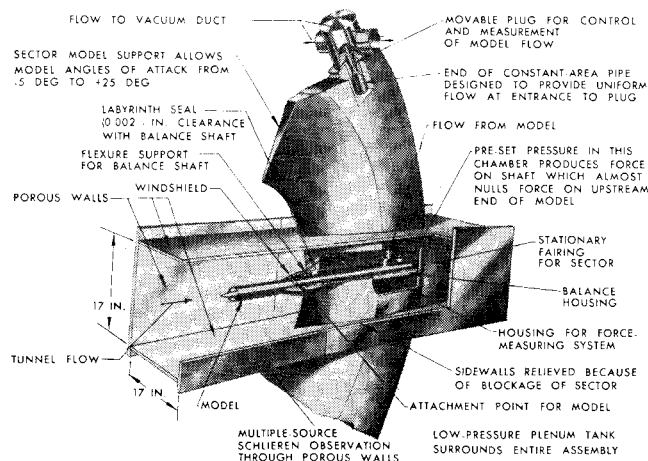


Fig. 2 Inlet model, balance, and support in 17-in. transonic wind tunnel.

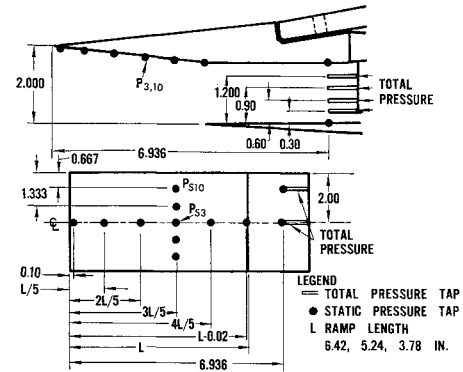


Fig. 3 Instrumentation diagram for two-dimensional inlet models.

### Measurement of Additive Drag

Since the terms and integration of Eq. (2) cannot be evaluated directly, additive drag must be measured indirectly. One method requires a test set up to measure the total force acting plus all other forces except additive drag. This method, illustrated in Fig. 1a, then yields additive drag

$$D_{add} = F_{bal} + (PA)_{base} - (PA)_{step} - m_0 V_0 - P_0 A_0 - D_f \quad (3)$$

$D_f$  is computed from flat-plate friction coefficient and is usually small. Mass flow is measured at the exit and equals

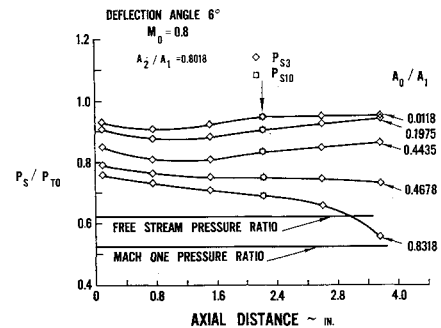


Fig. 4 Two-dimensional inlet ramp pressure distributions:  $M_0 = 0.8$ , 6° ramp, 0.802 area ratio.

$m_0$ . Freestream velocity ( $V_0$ ) and  $A_0$  are computed and all other terms measured directly. Another method that does not use a force balance measurement is shown in Fig. 1b. Here pressure instrumentation is used to determine forces acting between freestream and the inlet cowl so that additive drag is given by

$$D_{add} = D_{cb} + m_i \bar{v}_i + \bar{P}_i A_i - m_0 \bar{v}_0 - P_0 A_0 + D_f \quad (4)$$

The term  $D_{cb}$  is obtained by integrating the measured centerbody pressures over the centerbody area, and friction drag  $D_f$  is computed. Stream thrust at the throat

Table 1 Nominal test conditions

$M_0$	Total pressure, (psfa)	Reynolds number (4-in. capture diam)
0.5	4100	$1.97 \times 10^6$
0.8	4100	$2.66 \times 10^6$
0.85	4100	$2.75 \times 10^6$
1.1	4600	$3.41 \times 10^6$
1.3	6200	$4.57 \times 10^6$

Table 2 Test variables for two-dimensional inlets

Ramp angle	Throat-capture area ratio
6°	0.802
	0.723
	0.663
9°	0.701
	0.583
	0.492
12°	0.599
	0.440
	0.318

$(m_i \bar{v}_i + \bar{P}_i A_i)$  is the average obtained from throat measurements and the mass flow measurement. A computed or measured boundary-layer thickness can be used in evaluating stream thrust at the throat, but its influence is usually small.

Both methods were employed to evaluate additive drag in this study. Additive drag coefficient data are based on inlet capture area ( $A_1$ ) and is defined as

$$C_{D_{add}} = 2D_{add}/\gamma P_0 M_0^2 A_1 \quad (5)$$

### Test Techniques

#### Wind Tunnel

The inlet drag studies were conducted in the 17 × 17 in. transonic wind tunnel located at the United Aircraft Re-

Table 3 Test variables for axisymmetric inlets

Cone half-angle	Throat-capture area ratio
10°	0.80
	0.65
	0.50
14°	0.80
	0.65
	0.50
18°	0.80
	0.65
	0.50

search Laboratories. The tunnel is of the blow-down type with running times ranging from 0.5 to 1.5 min. The tunnel test section has porous walls that eliminate wall interference effects on the model. A Mach number range of 0.35 to 1.4 is available by adjusting the pressure in a plenum around the test section.

Figure 2 shows the test section of the wind tunnel. The inlet models are supported from the hydraulically actuated sector, which permits variation of the model angle of attack. A 12-in.-diam multiple-source schlieren system is used to obtain schlieren photos of the test models through the perforated walls. A complete description of the equipment and

Table 4 Test variables for 1959 inlet tests

Cone half-angle	Throat-capture area ratio
12°	0.45
	0.30
	0.15
16°	0.45
	0.30
	0.15
18°	0.45
	0.30
	0.15

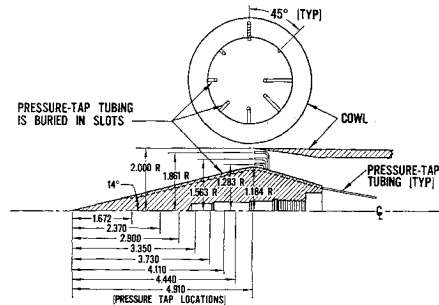


Fig. 5 Pressure tap installation for axisymmetric inlet model.

procedures used in the transonic wind tunnel is found in Ref. 4. Nominal test conditions are shown in Table 1. The total temperature was 540°R.

### Test Models

#### Two-Dimensional Inlets

A series of two-dimensional supersonic inlet models was tested. A sharp cowl having a straight 5° exterior shape was used on all models. Extended side plates having a 60° sweep angle were used. Three ramp angles were selected, each with three throat-capture area ratios, making nine configurations in all. Table 2 contains the test variables. Capture height was 2.0 in., and capture width was 4.0 in. All inlets were tested at Mach 0.5, 0.8, 1.1, and 1.3 at captured flow rates from choked to shutoff.

The pressure tap instrumentation is shown in Fig. 3. On the ramps, pressures were measured in the transverse direction at the mid-point to check the flow uniformity. In all cases, the transverse pressure distribution was uniform, indicating that no sideways flow existed as in Fig. 4. The same result was obtained at the throat measurement station. This indicated that the extended sideplates had performed their intended purpose of eliminating sideways flow spillage.

#### Axisymmetric Inlets

A series of axis symmetric inlets was tested. A sharp cylindrical cowl with a -5° straight interior shape was used on all models. Cowl diameter was 4 in. Conical centerbodies having three cone half-angles, each with three area ratios, were selected. The test variables are shown in Table 3. The inlets were tested at Mach 0.5, 0.85, 1.1, and 1.26 for the entire captured flow range. On one cone, pressure taps were installed, and a total pressure rake was used at

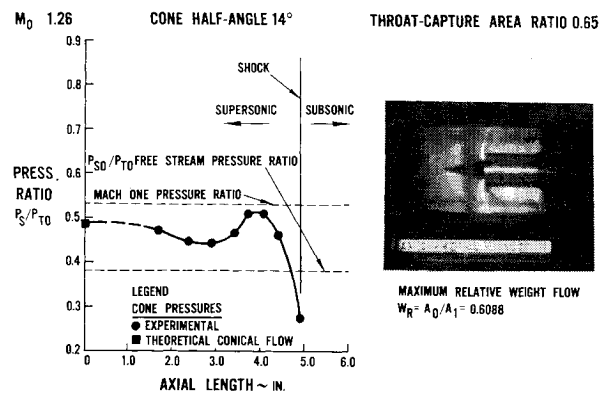


Fig. 6 Axisymmetric inlet cone pressure distribution and schlieren photo:  $M_0 = 1.26$ , 14° cone half-angle, 0.65 area ratio, maximum relative weight flow.

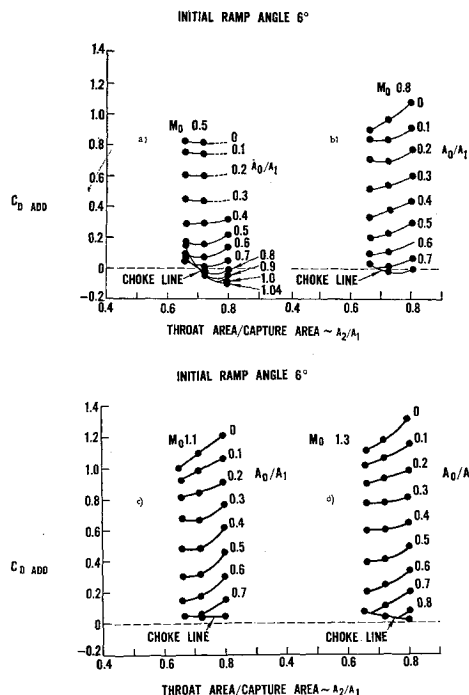


Fig. 7 Additive drag of two-dimensional supersonic inlets:  
a)  $M_0 = 0.5$ , b)  $M_0 = 0.8$ , c)  $M_0 = 1.1$ , d)  $M_0 = 1.3$ .

the throat. Figure 5 shows the setup. Thus, a check on the force-balance measurements was afforded.

The inlet models from the 1959 test series mentioned previously were geometrically similar to the present models except for the cone half-angles and area ratios. The cowl diameter was also different (4.7 in. instead of 4 in.). The variables are listed in Table 4. The 1959 models were tested at Mach 0.35, 0.6, 0.85, 1.0, and 1.22 over the entire flow range. Again, checks on the measurements were made by comparing force balance and pressure-tap drag results.

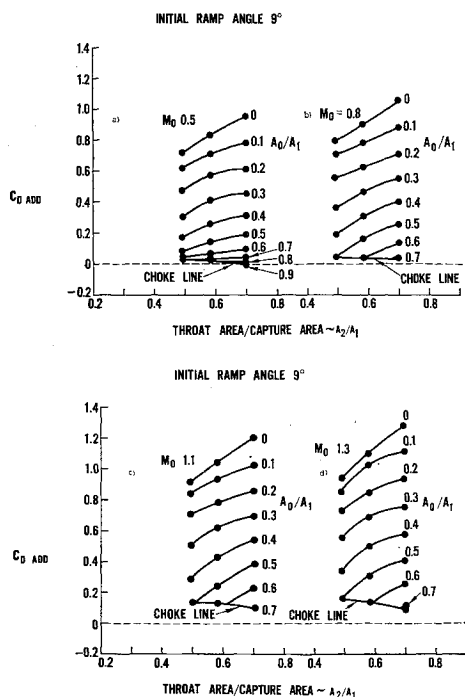


Fig. 8 Additive drag of two-dimensional supersonic inlets:  
a)  $M_0 = 0.5$ , b)  $M_0 = 0.8$ , c)  $M_0 = 1.1$ , d)  $M_0 = 1.3$ .

## Experimental Data

For the two-dimensional inlets, ramp pressure distributions were obtained so that the ramp drag could be computed. A typical set of pressures is shown in Fig. 4 for various flow rates at Mach 0.8 for a 6° ramp, 0.802 area ratio inlet. At subsonic speed, the pressure is high at the leading edge where the flow is turned and then drops off slowly. At high mass flows, the pressure is sharply reduced in a narrow region near the cowl lip station. As the mass flow decreases, the pressure along the entire ramp rises, although the pressure rise at the cowl station is the greatest. It may also be seen that the transverse pressure distribution is uniform, indicating two-dimensional flow.

Cone pressure distributions were also obtained for some of the axisymmetric inlet models. Some supersonic pressure distributions are shown in Fig. 6, accompanied by a corresponding schlieren photo of the flow.

Theoretical solutions for the subsonic drag of supersonic inlets are not available, as mentioned before. Thus, comparisons of subsonic drag data with theory cannot be made. The supersonic drag (attached shock), however, was checked against supersonic flow theory for supercritical operation. When the data were extrapolated to the theoretical maximum weight flow, the good agreement with supersonic flow theory is evident. A second check on the data was made by obtaining it using two methods. On one of the axisymmetric inlets, both axial force and pressure measurements were made. Good agreement between the two methods was obtained.

## Parametric Presentation of Additive Drag Data

The additive drag data for two-dimensional inlet configurations are shown in Figs. 7-9. The additive drag is plotted vs throat-capture area ratio for various relative weight flows. Data are shown for Mach numbers of 0.5, 0.8, 1.1, and 1.3 at ramp angles of 6°, 9°, and 12°.

Additive drag data for axisymmetric inlets are shown in Figs. 10-12. The data are plotted in the same manner as

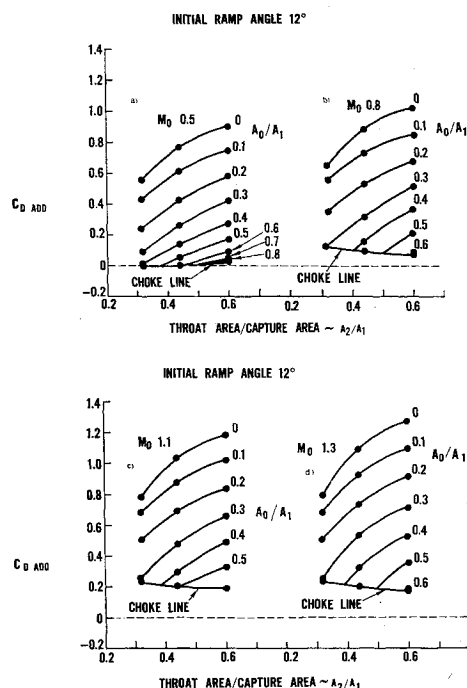


Fig. 9 Additive drag of two-dimensional supersonic inlets:  
a)  $M_0 = 0.5$ , b)  $M_0 = 0.8$ , c)  $M_0 = 1.1$ , d)  $M_0 = 1.3$ .

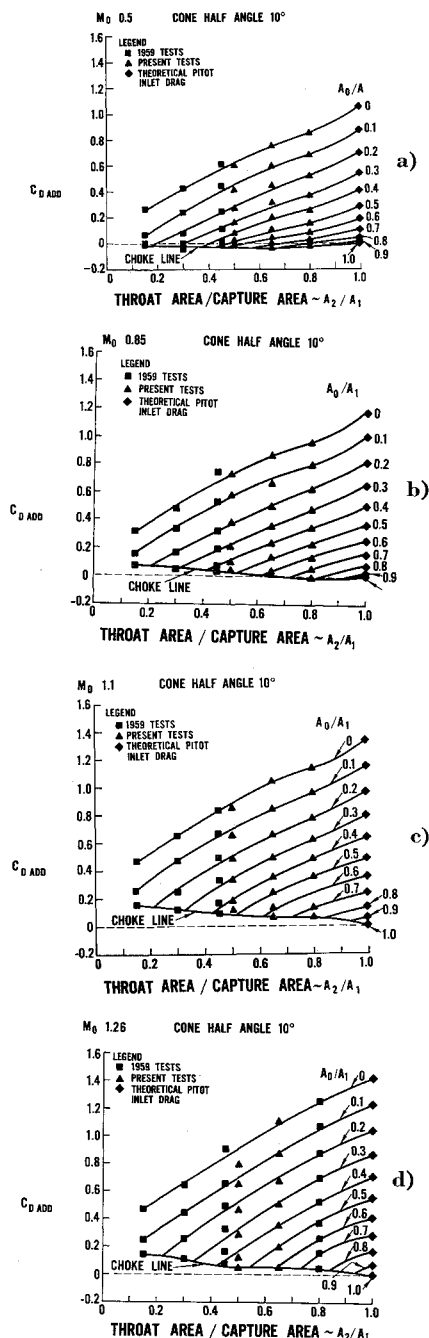


Fig. 10 Additive drag of axisymmetric supersonic inlets: a)  $M_0 = 0.5$ , b)  $M_0 = 0.85$ , c)  $M_0 = 1.1$ , d)  $M_0 = 1.3$ .

the two-dimensional inlet and are shown for Mach numbers of 0.5, 0.85, 1.1, and 1.26 at cone half-angles of  $10^\circ$ ,  $14^\circ$ , and  $18^\circ$ .

The data from the 1959 inlet tests were cross-plotted to obtain the curves shown here. In some of the curves, a systematic deviation of the 1959 data and the present data can be seen. The deviation is possibly because of differences in calibration of the instrumentation over the six-year interval between tests and to the necessary crossplotting. The data from both series were internally consistent as shown by the results of the force method and pressure method of obtaining additive drag.

Also plotted on the axisymmetric inlet curves are the theoretical predictions for pitot inlet additive drag.

It can be seen that the choked relative weight flow varies with Mach number. Intermediate values for choked-flow

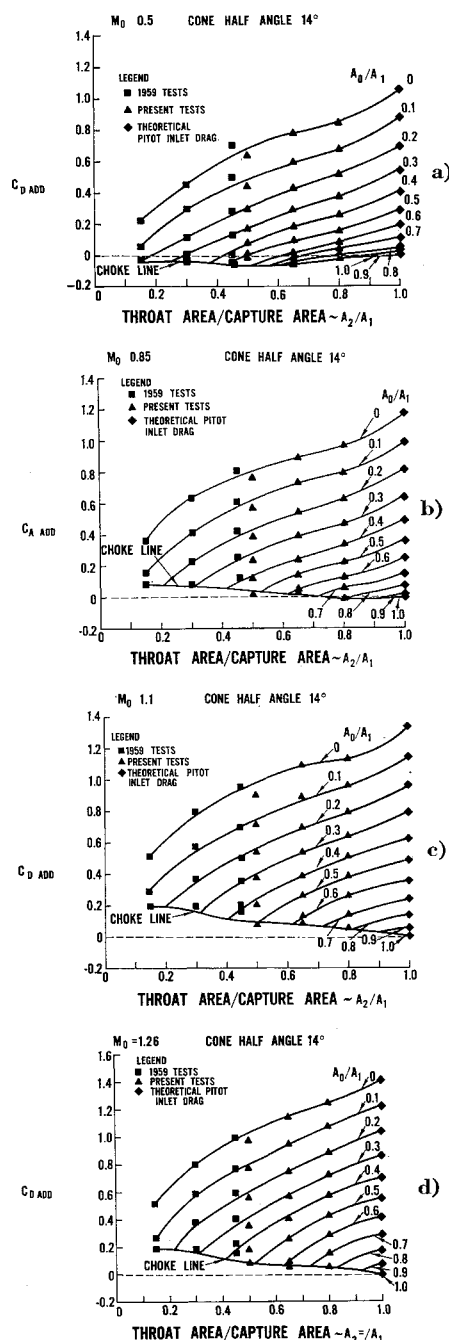


Fig. 11 Additive drag of axisymmetric supersonic inlets: a)  $M_0 = 0.5$ , b)  $M_0 = 0.85$ , c)  $M_0 = 1.1$ , d)  $M_0 = 1.26$ .

rate can be obtained by cross-plotting choked relative weight flow vs Mach number.

### Concluding Remarks

Additive drag data have been presented for subsonic and transonic operation of supersonic sharp-lipped inlets. Two-dimensional and axisymmetric inlets were studied in a systematic manner by varying the initial ramp or cone angle and the throat-capture area ratio. An inlet designer, using these parametric plots, can compute the drag in this Mach number range once the inlet design has been determined by design-point considerations.

The data show that sharp-lipped inlets should be designed for operation as near the choked-flow point as possible to reduce additive drag to a minimum. The data provide

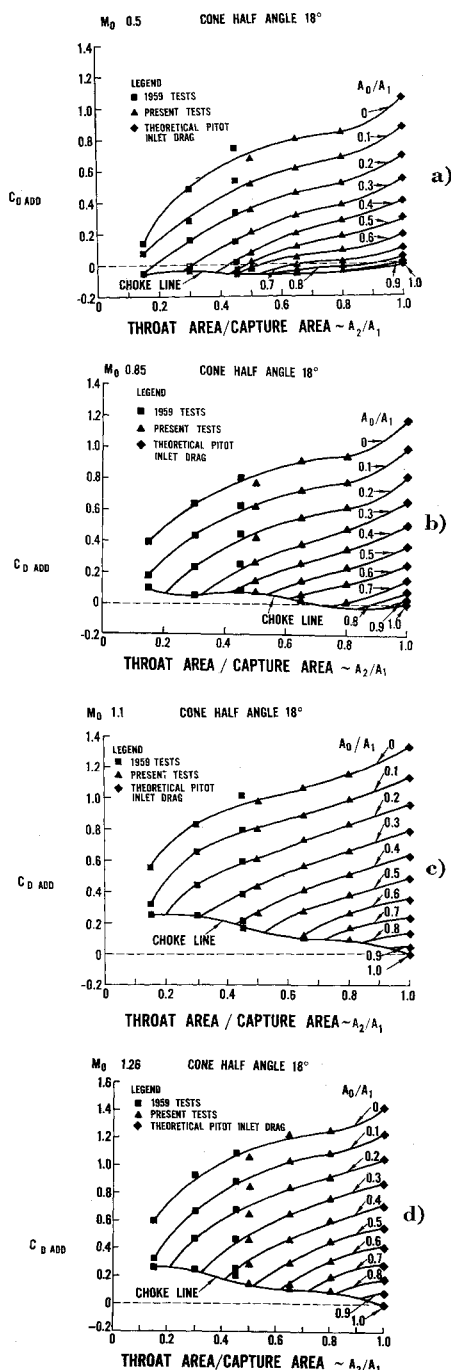


Fig. 12 Additive drag of axisymmetric supersonic inlets:  
a)  $M_0 = 0.5$ , b)  $M_0 = 0.85$ , c)  $M_0 = 1.1$ , d)  $M_0 = 1.26$ .

part of the information necessary to determine tradeoffs between pressure recovery (which affects engine thrust) and additive drag so that the optimum flow can be defined.

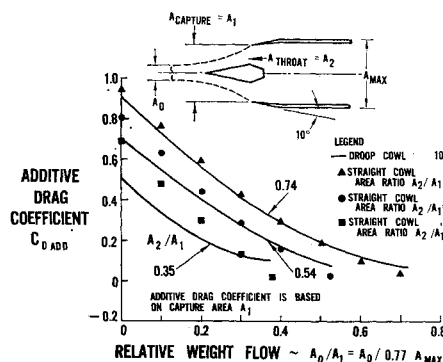


Fig. 13 Comparison between straight cowl and droop cowl additive drag.

At throat-capture area ratios of 0.7 or higher, it appears that the additive drag data have general application to any cowl configuration having a sharp lip when flow stagnation occurs inside the cowl. The influence of the cowl outer shape on the throat flow is small for these cases. The reasons for this are that a separated flow region exists on the outside of the cowl lip, thus masking its shape, and that the local region of cowl shape influence is small compared to the throat height. A comparison between cylindrical cowl data and data for a  $10^\circ$  straight cowl<sup>5</sup> is shown in Fig. 13.

The data presented also show that the subsonic and transonic additive drag of two-dimensional inlets is higher than axisymmetric inlets when the initial ramp or half-cone angle and throat-capture area ratio are the same. The same thing happens at supersonic speed as other investigators have found. In subsonic flow, the flow is diverted in one direction by a wedge and in two directions by a cone. Thus, for equal wedge and half-cone angles, curvature of the flow is sharper in the wedge case, and centrifugal forces raise the wedge pressure higher than in the case of the cone.

The additive drag rise with decreasing relative weight flow is roughly linear for the Mach 0.8 to 1.3 range. The exception to this rule occurs at low relative weight flows and at Mach 0.5.

## References

- Mount, J. S., "The effect of inlet additive drag on aircraft performance," AIAA Paper 64-599; also J. Aircraft 2, 374-378 (1965).
- Motycka, D. L., "Results of subsonic and transonic additive drag test," Pratt & Whitney Aircraft Internal Memo (June 1959).
- Sibulkin, M., "Theoretical and experimental investigation of additive drag," NACA Rept. 1187 (1954).
- McLafferty, G. and Vergara, R., "Description of equipment and techniques used for inlet tests in UAC research department 17-inch blowdown tunnels," UAC Research Laboratories Rept. R-2000-30 (July 1957).
- Muller, G. L. and Gasko, W. F., "Studies of drag-reduction methods for subsonic operation of supersonic inlets," Pratt & Whitney Aircraft TDM 1974 (May 1966); also J. Aircraft (submitted for publication).